level, the SVC_I-VR model's predictions do not match available experiment data for a number of tested paradigms (i.e., somatogravic illusion, tilt perception in a centrifuge). All motion perception paradigm data are accurately matched by the tested MSOM-VR + VV, which includes both visual rotational velocity and visual orientation perception, however, no correct frequency sensitivity of motion sickness is shown in the MSOM. Thus, the performed model comparison shows that no single model exists that can accurately predict the effects of vision on motion sickness and motion perception. Our next steps include expanding our model comparison effort to include other conflict terms such as in (Allred and Clark 2023). Here we expect the model by Allred and Clark (2023) to provide results similar to our results for the MSOM when comparing the predicted conflicts. The main improvement comes from the use of the nonlinear function by Oman (1990) which greatly improves the motion sickness frequency dynamics as shown in Kotian et al (2023). Crucial steps towards realizing such a unified model are, based on the analysis in this paper, the implementation of more complete otolith-semicircular canal interactions in SVC-based models such as the SVC_I-VR, adding a band-pass filter to correct the frequency dynamics of the MSOM. Along with this, future experiments will be directed towards addressing the gaps in the existing literature identified in this study.

Appendix A: Additional simulations

Vision parameter sensitivity

Figures 16, 17, 18 show the vision loop gain parameter sensitivity for all three models, i.e., SVC_I, SVC_{NI}, and MSOM. The feedback gains for both the vision loops (*visual rotational velocity* and *visual vertical*) are varied from 0 to 20

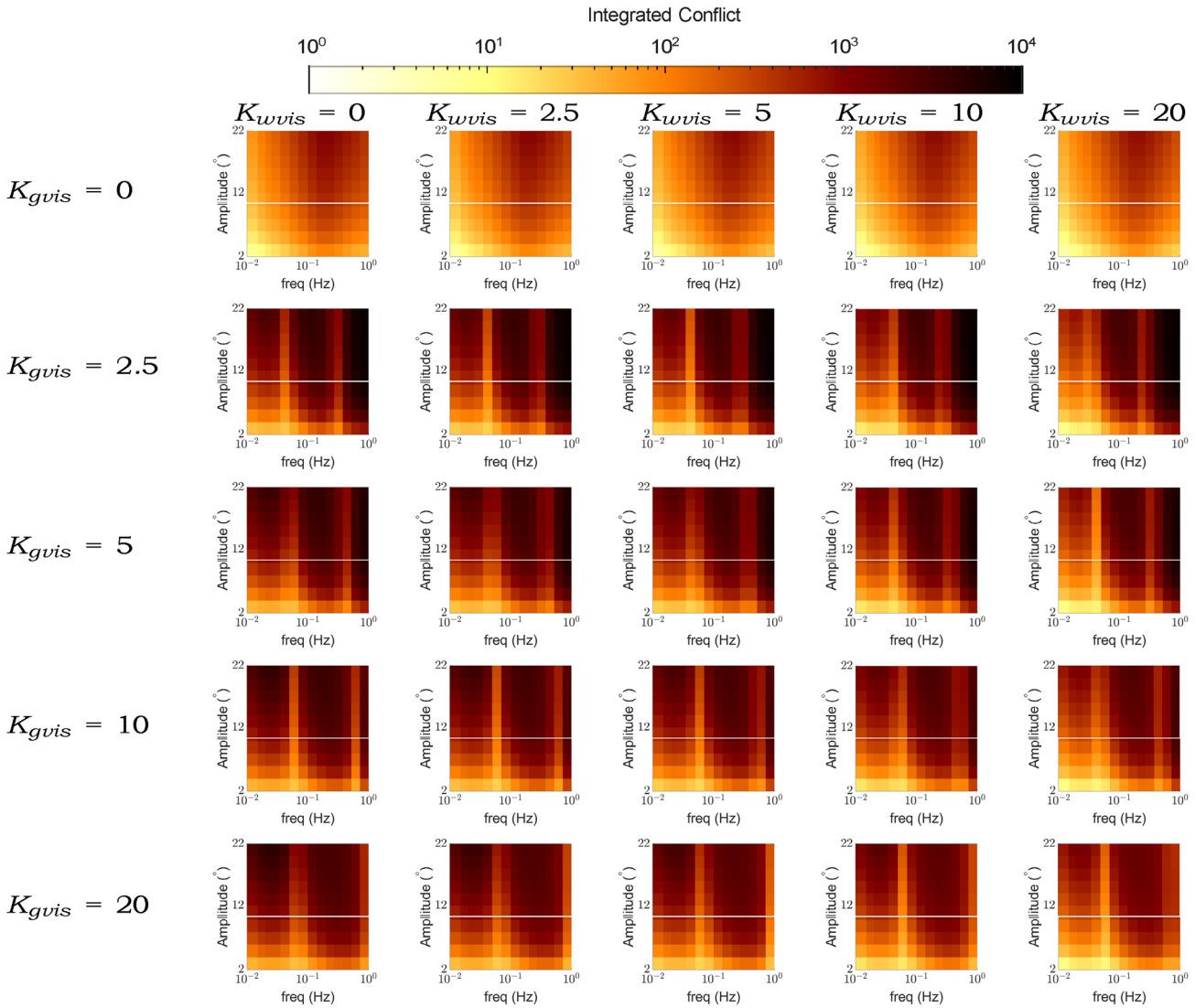

Fig. 16 Frequency sensitivity of integrated conflict with sinusoidal pitch oscillations for varying values of K_{wvis} and K_{gvis}, for the SVC_I model

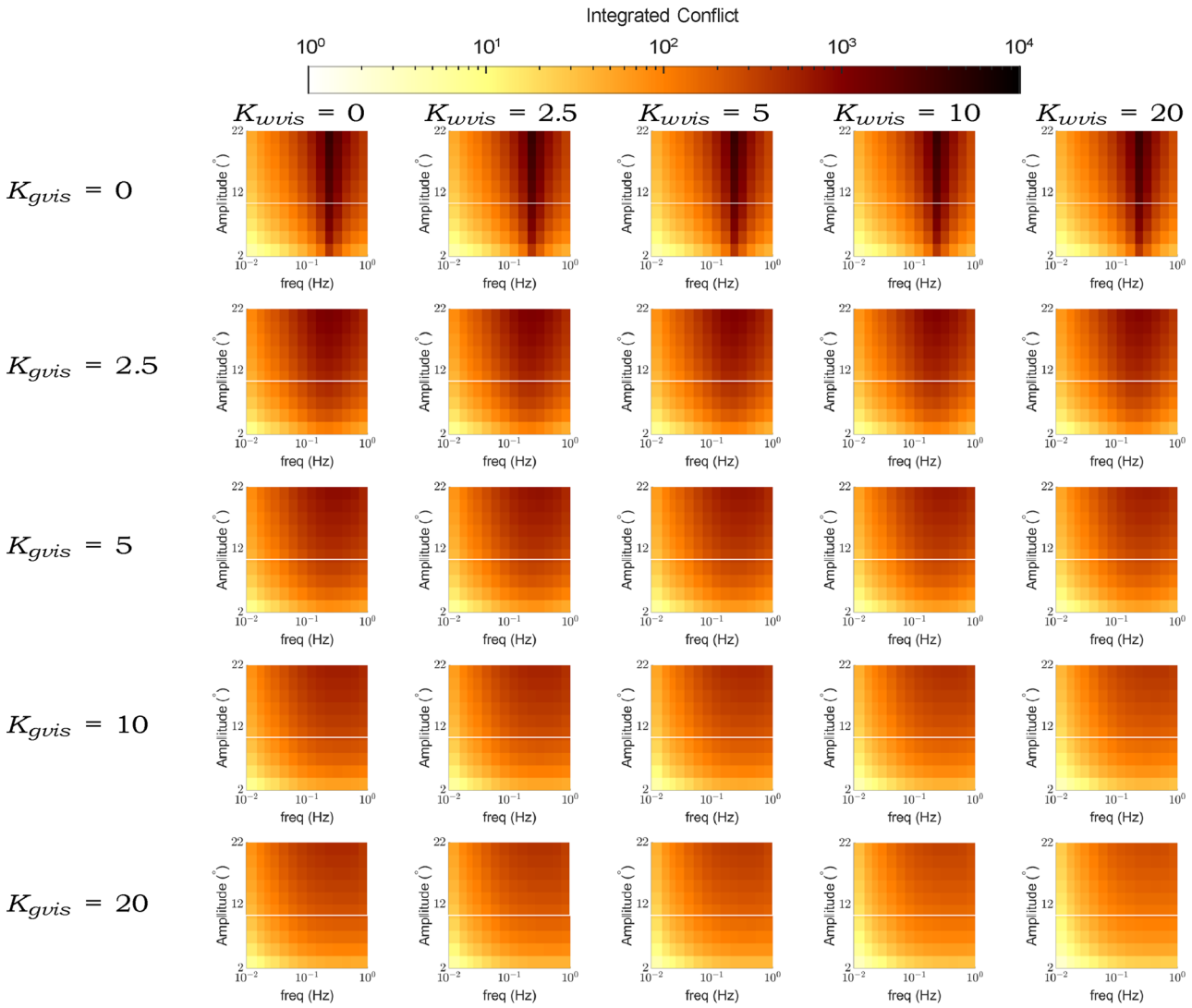

Fig. 17 Frequency sensitivity of integrated conflict with sinusoidal pitch oscillations for varying values of K_{wvis} and K_{gvis}, for the SVC_{NI} model

and the frequency and amplitude sensitivity responses for sinusoidal pitch oscillations with 'external vision'.

In the SVC_I model, it is observed in Fig. 16 that a higher gain for the *visual vertical* shifts the peak conflict frequency to a higher frequency. As K_{gvis} approaches 20, the peak conflict frequency approaches 0.5 Hz. On the other hand, a higher gain for *visual rotational velocity* (K_{wvis}) only reduces the conflict levels by providing correct estimates of pitching oscillations, which is the simulated input.

Figure 17 shows the effect of K_{wvis} and K_{gvis} on the SVC_{NI} model. The effects are similar to effects in the SVC_I model where, higher gains for the *visual vertical* move the peak conflict frequency to higher frequencies (around 0.5 Hz), while higher gains on the *visual rotational velocity* conflict reduce the conflict levels.

In the MSOM, the use of *visual rotational velocity* reduces the magnitude of conflict, see Fig. 18. The higher the gain on the *visual rotational velocity* (K_{wv}), the higher the reduction of conflict. The *visual vertical* feedback gain setting also has a similar effect on conflict. The higher the gain on the *visual vertical* (K_{wv}), the higher the reduction of conflict. Also, as seen in Sect. 3.3, the *visual vertical* does help in motion perception tests.

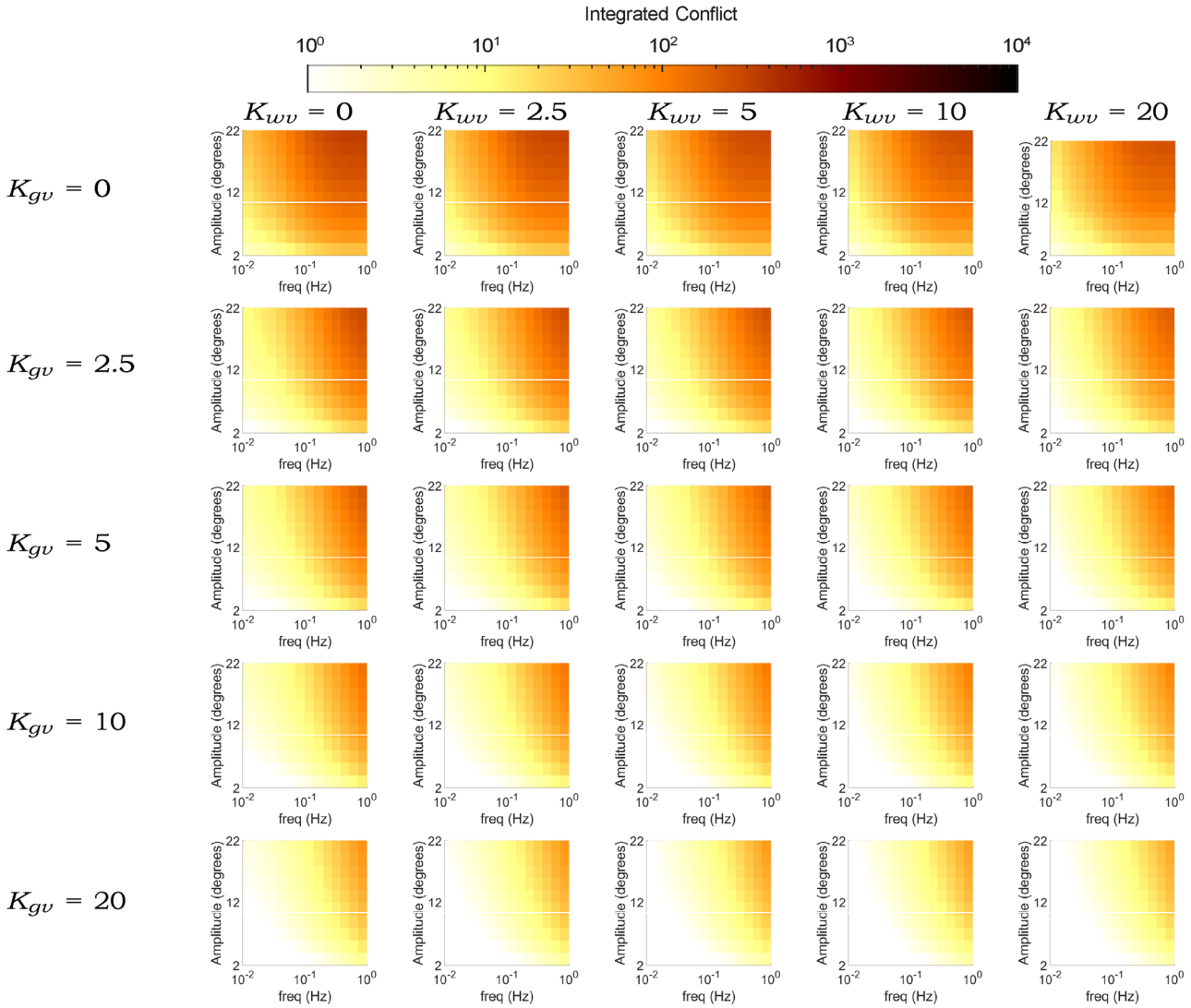

Fig. 18 Frequency sensitivity of integrated conflict with sinusoidal pitch oscillations for varying values of K_{wv} and K_{gv}, for the MSOM model

Pure yaw simulations

As discussed in Sect. 3.1.2, pure yaw rotations lead to no verticality conflict generation in any of the three models. This is due to the pure yaw motion not having any effect on the verticality vector. There are other conflict terms in the models that do get affected by pure yaw motion, however, these terms are not used for sickness predictions in our study. This absence of motion sickness holds true even with the presence of vision. Figure 19 shows that different amplitudes of sinusoidal yaw at different frequencies show no motion sickness (zero conflict generation) and are thereby not visible in plots.

Slalom drive

Here, the aim was to analyze the effect of the applied motion DOF on the magnitude of conflict which then in turn tells us about the sensitivity of motion sickness to each of these degrees of freedom. This will demonstrate the effect of the visual pathways for different motion degrees of freedom. The inputs, being real-world slalom drive data, are not identical for all degrees of freedom, it has high levels of lateral accelerations and yaw velocities. Hence, it is expected that different degrees of freedom will result in

Fig. 19 Frequency sensitivity of integrated conflict with sinusoidal yaw oscillations for different vision conditions: 'no vision' (eyes closed), 'external vision' (eyes open and with outside view), 'internal vision' (eyes open and without outside view), 'only vision' (no motion) for the SVC_I, SVC_{NI} and MSOM model

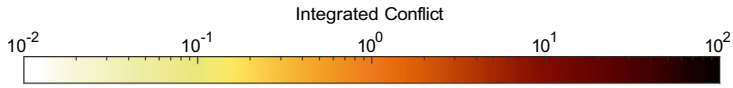

Names	No Vision	External Vision	Internal Vision	Only Vision
SVC_I-VR				
SVC_I-VV				
SVC_I-VR+VV				
SVC_{NI}-VR				
SVC_{NI}-VV				
SVC_{NI}-VR+VV				
MSOM-VR				
MSOM-VV				
MSOM-VR+VV				

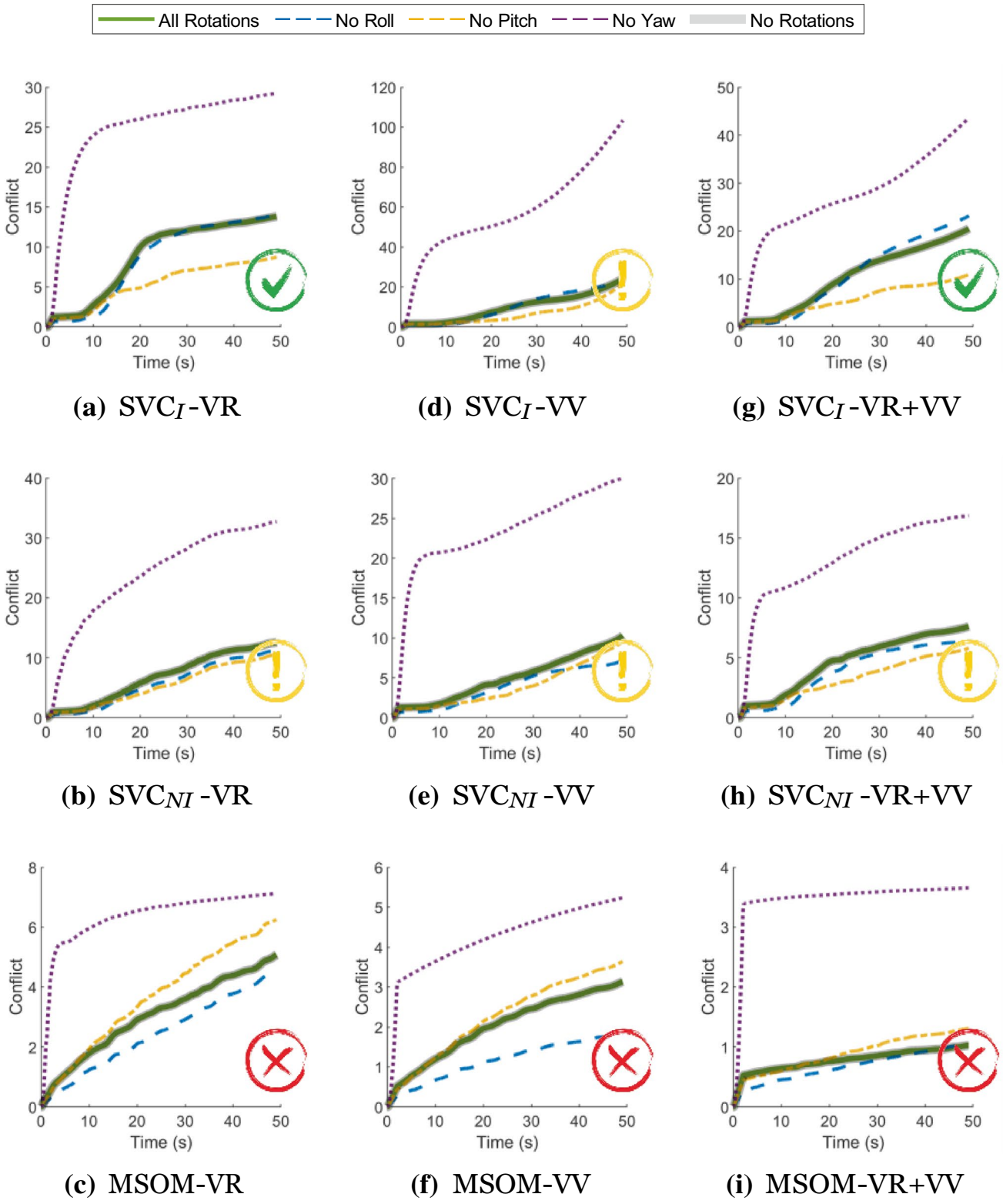

Fig. 20 Effect of rotational DOF on the conflict in the slalom drive

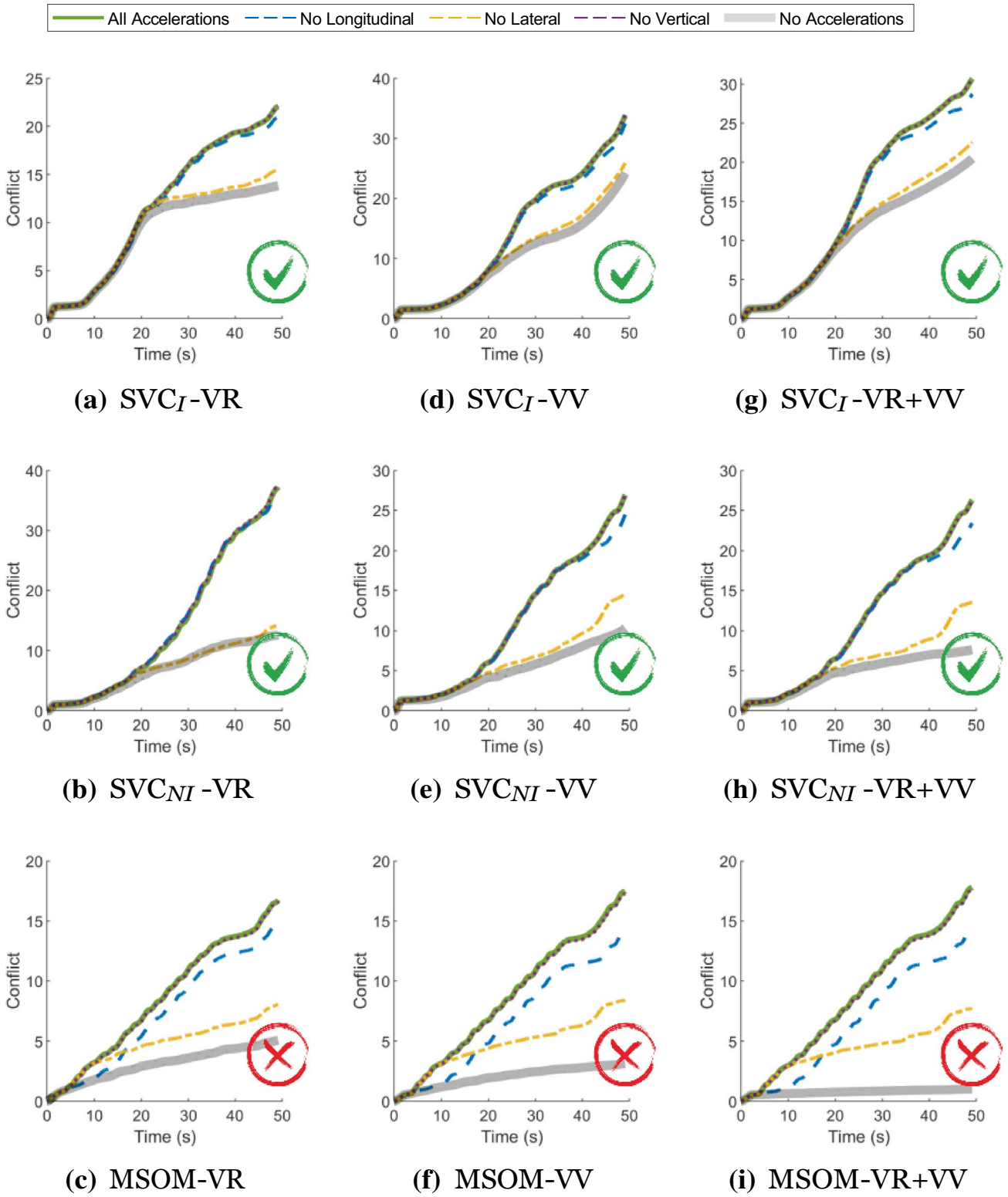

Fig. 21 Effect of linear acceleration on conflict in the slalom drive

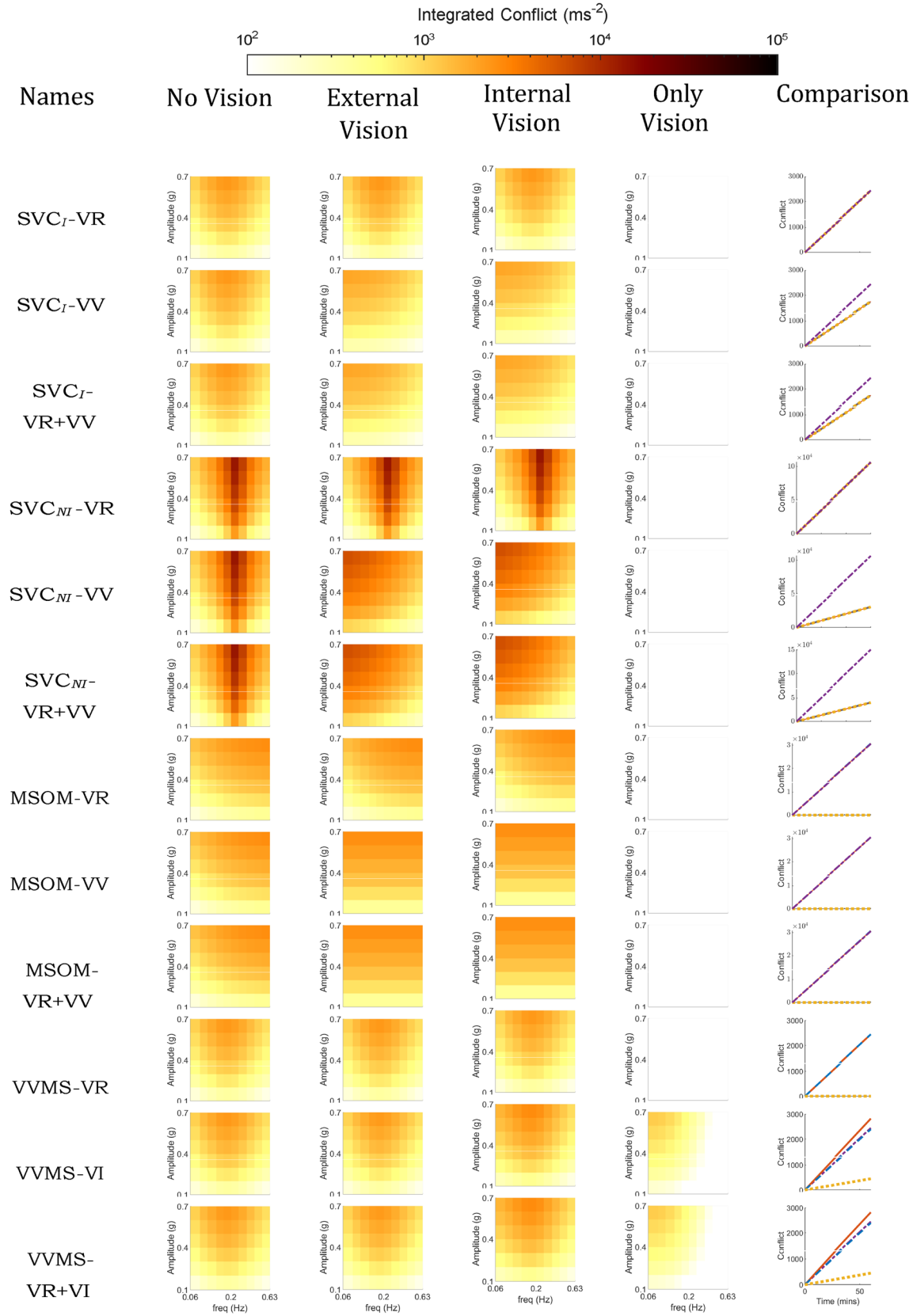
Integrated Conflict (ms-2)
10^2
10^3
10^4
10^5
Names
No Vision
External Vision
Internal Vision
Only Vision
Comparison
SVC_I-VR
SVC_I-VV
SVC_I-VR+VV
SVC_NI-VR
SVC_NI-VV
SVC_NI-VR+VV
MSOM-VR
MSOM-VV
MSOM-VR+VV
VVMS-VR
VVMS-VI
VVMS-VR+VI
Amplitude (g)
freq (Hz)
Conflict
Time (mins)

◂**Fig. 22** Frequency sensitivity of integrated conflict (ms^{-1}) with sinusoidal fore-aft motion for different vision conditions: 'no vision' (eyes closed), 'external vision' (eyes open and with outside view), 'internal vision' (eyes open and without outside view), 'only vision' (no motion) and comparison of vision cases at 0.2 Hz and 0.7 g fore-aft motion for SVC_I, SVC_{NI} and MSOM (plots for the 'no vision' case are the same as in Fig. 4)

different conflicts. Thus, on the removal of lateral accelerations or yaw velocities, it is expected that the conflict will greatly change. To make these comparisons, in the following sections, each degree of freedom will be turned off and compared with cases of all degrees of freedom turned off and on.

Effects of individual axis rotations

In this analysis, the rotational degrees of freedom are set to zero one by one. The translational degrees of freedom are left active. This is shown in Fig. 20, where for each rotational degree of freedom all visual and vestibular signals are set to zero to quantify their contribution to the models' predictions. For reference, these effects are also compared with cases where all the rotation DOFs are removed and where all are active. The input data have strong yaw motion throughout the slalom drive. Pitch and roll are also present throughout the drive, however, their magnitudes are much lower than the yaw. As yaw is the dominant rotation, it is expected that the removal of yaw will significantly influence conflict. The roll provides compensation of sensed vertical in the lateral direction and hence its removal will decrease conflict due to decreased error in the estimation of vertical in the *Y*-direction. The longitudinal accelerations are of a lower magnitude to induce any pitch and hence, removal of pitch is expected to have small effect on conflict.

For the SVC_I model, it is observed that the removal of the yaw indeed has the strongest effect (of increasing conflict) in all versions. This is followed by the pitch, which results in a moderate reduction in conflict. Roll has a very low effect on the SVC_I-VR model. However, it increases conflict in models with *visual vertical* (VV). This is due to a better estimate of vertical through *visual vertical* in absence of roll.

For SVC_{NI} models, it is also observed that the removal of the yaw has the most effect (of increasing conflict) in all versions. However, the effect is most prominent in the model with only *visual rotational velocity*. The *visual vertical* reduces the spread of the different vision conditions.

For the MSOM, it is also observed that the removal of the yaw has the most effect (of increasing conflict) in all versions. Removal of pitch leads to a small increase in conflict. On the other hand, the removal of roll leads to a small decrease in conflict. However, the magnitude of conflict is still less than in the SVC models, see Fig. 20. This is because the conflict selected is the otolith conflict, which was proposed to correlate best with sickness (Irmak et al. 2023).

For all six models, yaw motion strongly affected conflict in complex 3D motion, highlighting the importance of using recorded or simulated head yaw in motion sickness predictions. This result is only found in the slalom drive whereas pure yaw did not elicit any conflict as described in appendix A.2.

From the results of all six models, it is evident that the MSOM is not suitable as a conflict generation model when strong rotations are present. The SVC_I models are able to perform as expected with the most dominant rotations in the slalom drive data having the most effect on conflict. Thus, SVC_I models are a better choice for simulations of human body rotations.

Effects of individual linear accelerations

In the previous section, the effects of each rotation on the models' sickness predictions for the slalom drive data were studied. Similarly, in this section, the effect of different linear DOFs will be studied while including all rotations. As in the previous section, each DOF is excluded and the data from the experiment is simulated. The results for the predicted conflict accumulation are shown in Fig. 21.

The input data have large lateral accelerations (around 4 ms^{-2}) and that too for a larger duration than other linear accelerations. Longitudinal accelerations are mostly present at the start and end of the drive. Finally, the vertical accelerations are of very low magnitude (less than 1 ms^{-2}). Thus, it is expected that the removal of longitudinal or vertical accelerations will not result in appreciable changes in conflict. Only the absence of lateral accelerations will produce a decrease in conflict.

In the SVC_I model, it is observed that the removal of lateral accelerations reduces conflict. Removal of longitudinal or vertical accelerations has very little effect on conflict accumulation due to their small magnitudes. These results imply that the linear degrees of freedom do have a large effect in models on SVC_I model.

For the SVC_{NI} model, the results are consistent across the three different versions: the removal of lateral accelerations has the most effect (of reducing conflict), followed by the removal of longitudinal accelerations. The omission

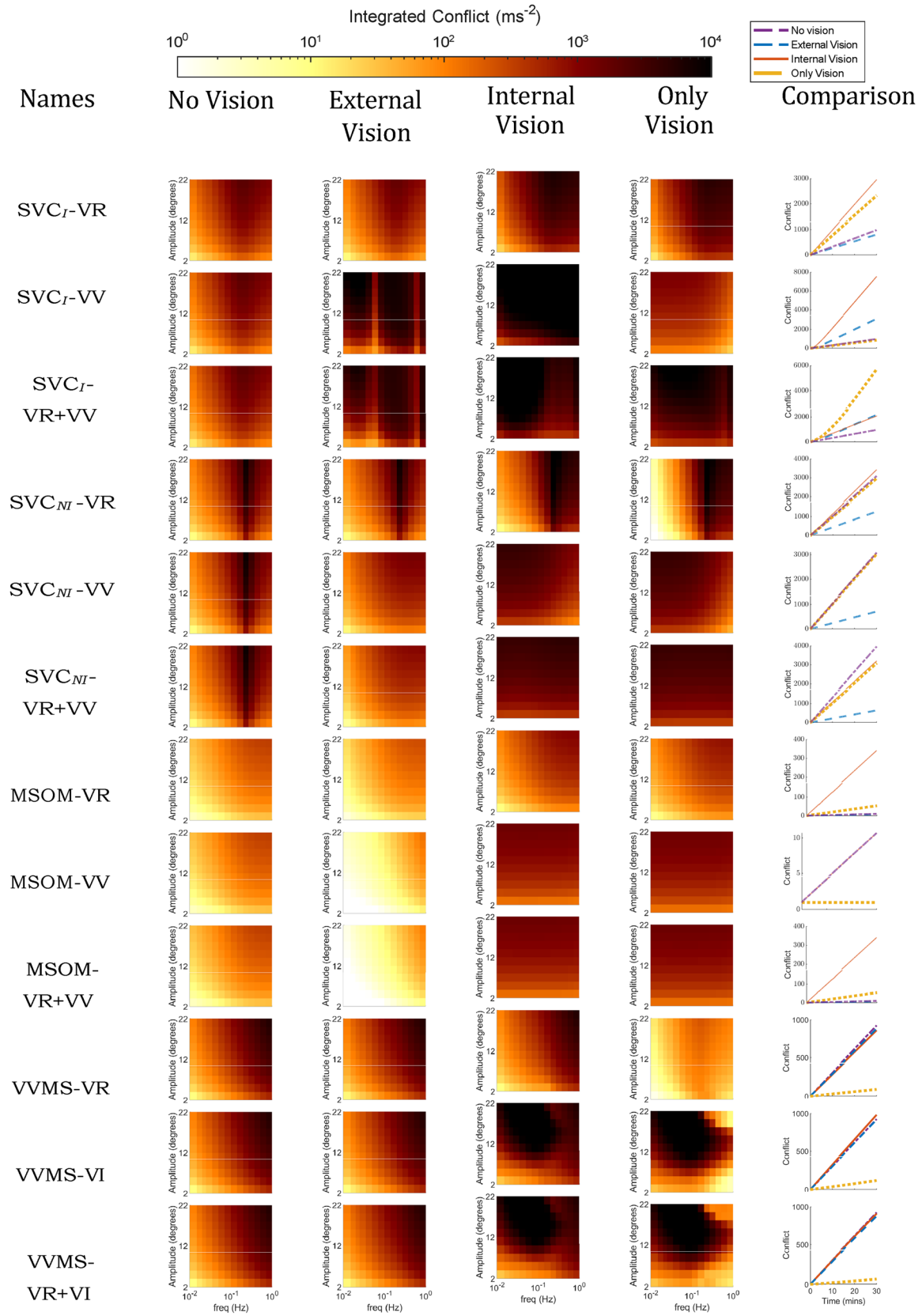
Integrated Conflict (ms-2)
10^0
10^1
10^2
10^3
10^4
No vision
External Vision
Internal Vision
Only Vision
Names
No Vision
External Vision
Internal Vision
Only Vision
Comparison
SVC_I-VR
SVC_I-VV
SVC_I-VR+VV
SVC_NI-VR
SVC_NI-VV
SVC_NI-VR+VV
MSOM-VR
MSOM-VV
MSOM-VR+VV
VVMS-VR
VVMS-VI
VVMS-VR+VI
Amplitude (degrees)
freq (Hz)
Conflict
Time (mins)

◂**Fig. 23** Frequency sensitivity of integrated conflict (ms^{-1}) with sinusoidal pitch motion for different vision conditions: 'no vision' (eyes closed), 'external vision' (eyes open and with outside view), 'internal vision' (eyes open and without outside view), 'only vision' (no motion) and comparison of vision cases at 0.2 Hz and 20° pitch motion for SVC_I , SVC_{NI} and MSOM

of vertical accelerations only has no effect on the conflict. These results are as expected.

In the MSOM, it is observed that the variations in conflict accumulation due to switching off the accelerations are greater than due to switching off the rotations. When no linear accelerations and only rotations are applied, MSOM reports very low conflicts. This indicates that the conflict in MSOM is heavily dependent on linear accelerations and not on rotations. When the lateral accelerations are removed, there is a strong reduction in conflict. However, when the vertical acceleration input is disabled, no change in conflict compared to the 'all accelerations' case is observed. Longitudinal accelerations have an intermediate effect.

From these results, it is evident that the otolith conflict term in the MSOM very strongly depends on linear degrees of freedom, while conflict from SVC_I and SVC_{NI} models have a very low dependency on the linear degrees of freedom. Of all the models, only the SVC_I-VR and all of the SVC_{NI} models are able to match the desired results.

B: Visual-Vestibular Motion Sickness (VVMS) model

The Visual-Vestibular Motion Sickness (VVMS) model, a variation of the SVC model developed by Jalgaonkar et al. (2021), Sousa Schulman et al. (2023), incorporates visual inputs based on the non-linear visual-vestibular interaction model proposed by Telban and Cardullo (2001). It includes the 'visual rotational velocity' ('VR'), similar to SVC and MSOM models, and introduces 'visual inertia' ('VI'). However, at this moment the VVMS model lacks empirical validation and raises doubts about its physiological basis due to human limitations in visually perceiving acceleration (Gottsdanker 1956; Werkhoven et al. 1992).

Testing the VVMS model alongside the other models in our comparison revealed its peculiar results in motion sickness and perception tests (Appendices B.1 and B.2). We have used the parameters as published in Sousa Schulman et al. (2023). Appendix B shows that sickness results are identical to the SVCI -VR without vision, but adding vision marginally affects sickness results. Consequently, the VVMS model, in its current state, is not preferable for motion perception or sickness predictions. The conclusion of the paper remains unaffected by its inclusion in our comparison (late in the publication process), as the SVC-VR and MSOM-VR + VV models remain superior for predicting motion sickness and perception, respectively.

B.1 Motion sickness

Sickness with head translation

Figure 22 shows that the responses for the VVMS model are identical to the SVCI -VR model. This figure is an extension of figure 6. It can also be noted that the effect of vision is small on the integrated conflict for the cases with physical motion ('external', 'internal' and 'no' vision). The absence of motion sickness in 'only vision' case for the VVMS-VR is consistent with all other models. However, VVMS-VI and VVMS-VR+VI do show sickness at low frequencies. Despite the promise shown by VVMS models utilizing 'VI' inpredicting sickness during pure translation, it is critical to acknowledge that humans do not possess the ability to perceive visual inertia.

Sickness with head rotation

The conflict accumulation can be seen in Fig. 23 for motion sickness with rotations. This figure is an extension of Fig. 7. The VVMS model gives a high-pass response with more motion sickness at higher frequencies. This behaviour remains the same for 'no' and 'external' vision conditions across all variations in the VVMS model (VR, VI, VR+VI). In the VVMS-VR model, the 'internal' and 'only' vision conditions too show the sane high pass dynamics but with 'only' vision having very low levels ofconflict and also a different peak frequency. For the VVMS models with 'VI', a very different frequency and amplitude dynamics is seen where the peak frequency decreases with increase in amplitude. This may be due to an occurrence of resonance at particular frequencies and amplitudes.

B.2 Motion perception paradigm tests

We have queried the same signals as the other SVC models in our comparison.

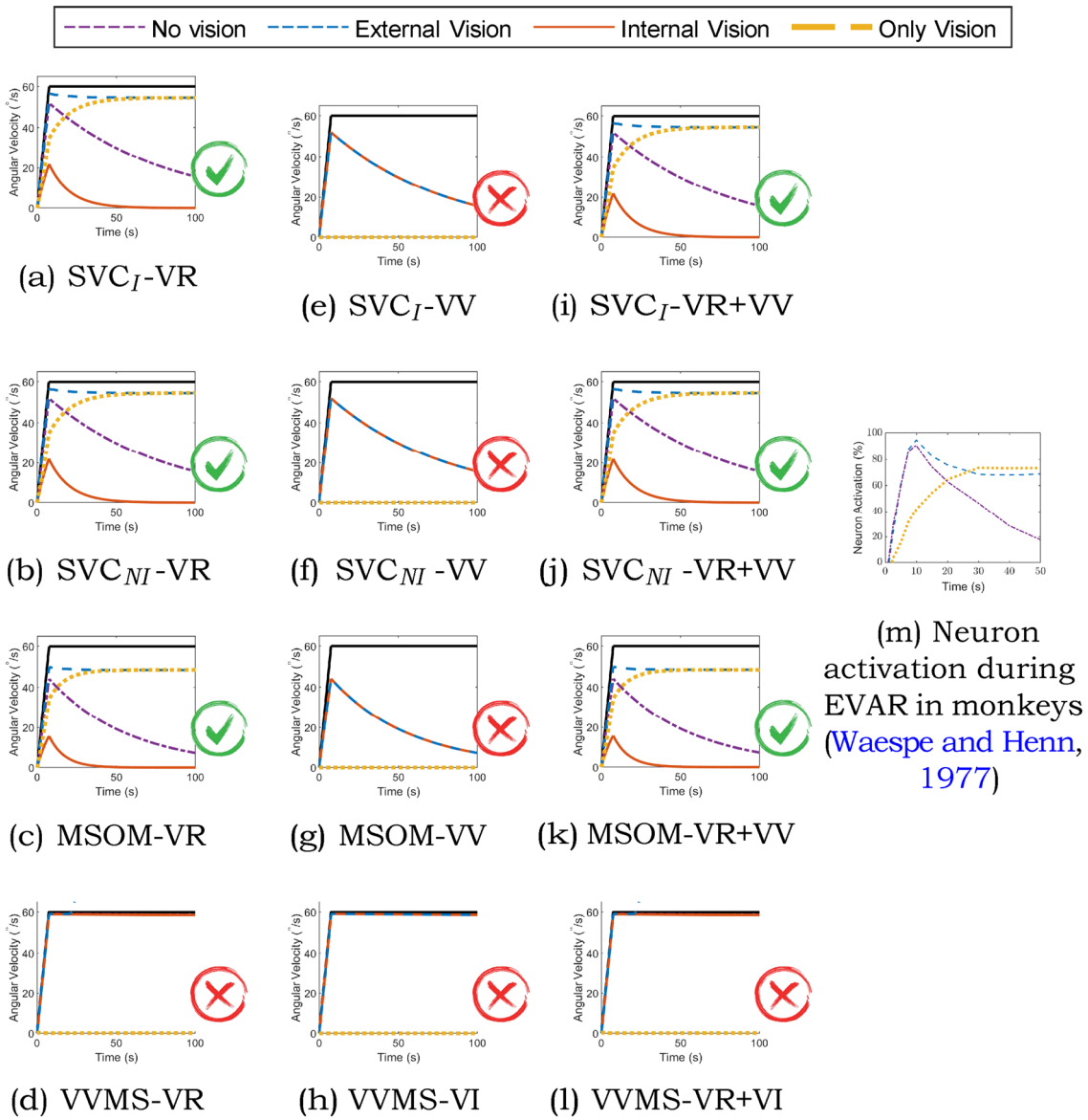

Fig. 24 Angular velocity perception during EVAR at 60 s^{-1};Red cross—result in disagreement with literature, Green Tick—result in agreement with literature

EVAR (Earth Vertical Axis Rotation) and OVAR (Off-Vertical Axis Rotation)

Figure 24 shows the yaw angular velocity perception to stimuli of EVAR at 60 s^{-1}. The VVMS model gives a perfect perception of yaw velocity in cases with physical motion ('external', 'internal' and 'no' vision cases). However, there is no perception of rotational velocity in 'only vision' case, where there is no physical motion. This is not what was expected and seen in Waespe and Henn (1977).

Somatogravic illusion

The results for all the variations of the VVMS model (see Fig. 25) are iden- tical to the results of the SVCI -VR model. This means there is no effect of these visual inputs on responses to somatogravic illusion.

Centrifugation

The VVMS's response to inputs representative of centrifugation are shown in Fig. 26. The response for the first 30 s

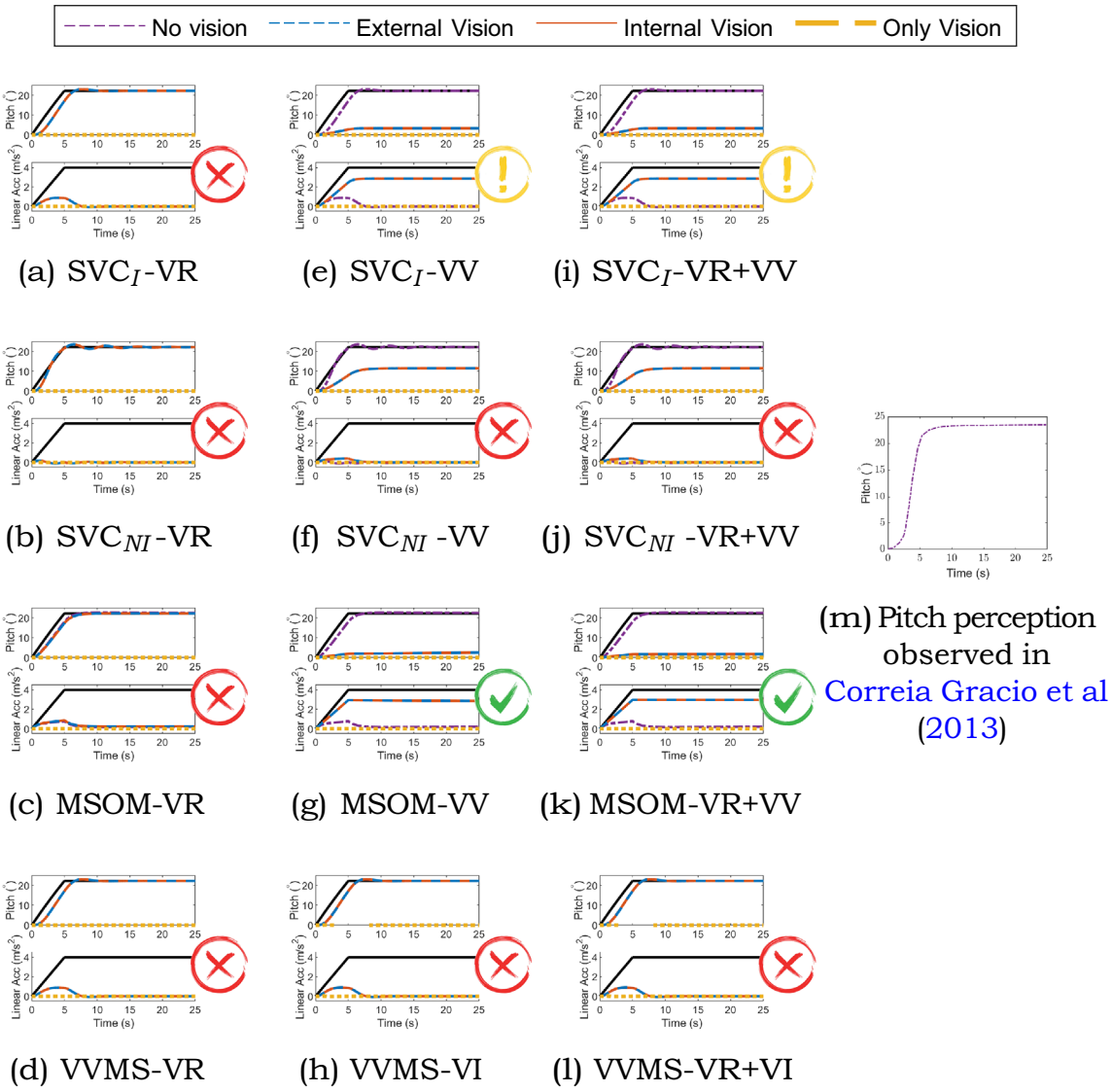

Fig. 25 Pitch perception during constant acceleration of 4 ms^{-2} (somatogravic illusion); For each condition the upper graph shows the perceived pitch and the lower graph the perceived acceleration. Black lines describe the applied acceleration in the lower graph, and the equivalent rotation in the upper graph.Red cross—result in disagreement with literature, Green Tick—result in agreement with literature, Yellow Exclamation—some of the results are in agreement with literature

is identical in all three variations of VVMS mode (VR, VI, VR + VI). However, the magnitude of the perceived roll-tilt is underestimated. Also, the VVMS model estimates that this illusion occurs in all conditions with physical motion, regardless of the vision condition. After around 40 s, the responses for the external vision case for the VVMS-VR and VVMS-VR + VI models become unstable. This could be because of the late addition of visual cues, which is, in turn, due to the delays that are present in the model for visual cues.

B.3 Motion sickness predictions for real-world sickening drive

Figure 27 shows the integrated subjective vertical conflict generated due to slalom manoeuvre (Irmak et al. 2020), as introduced in Sect. 2.2, by all the models for the considered

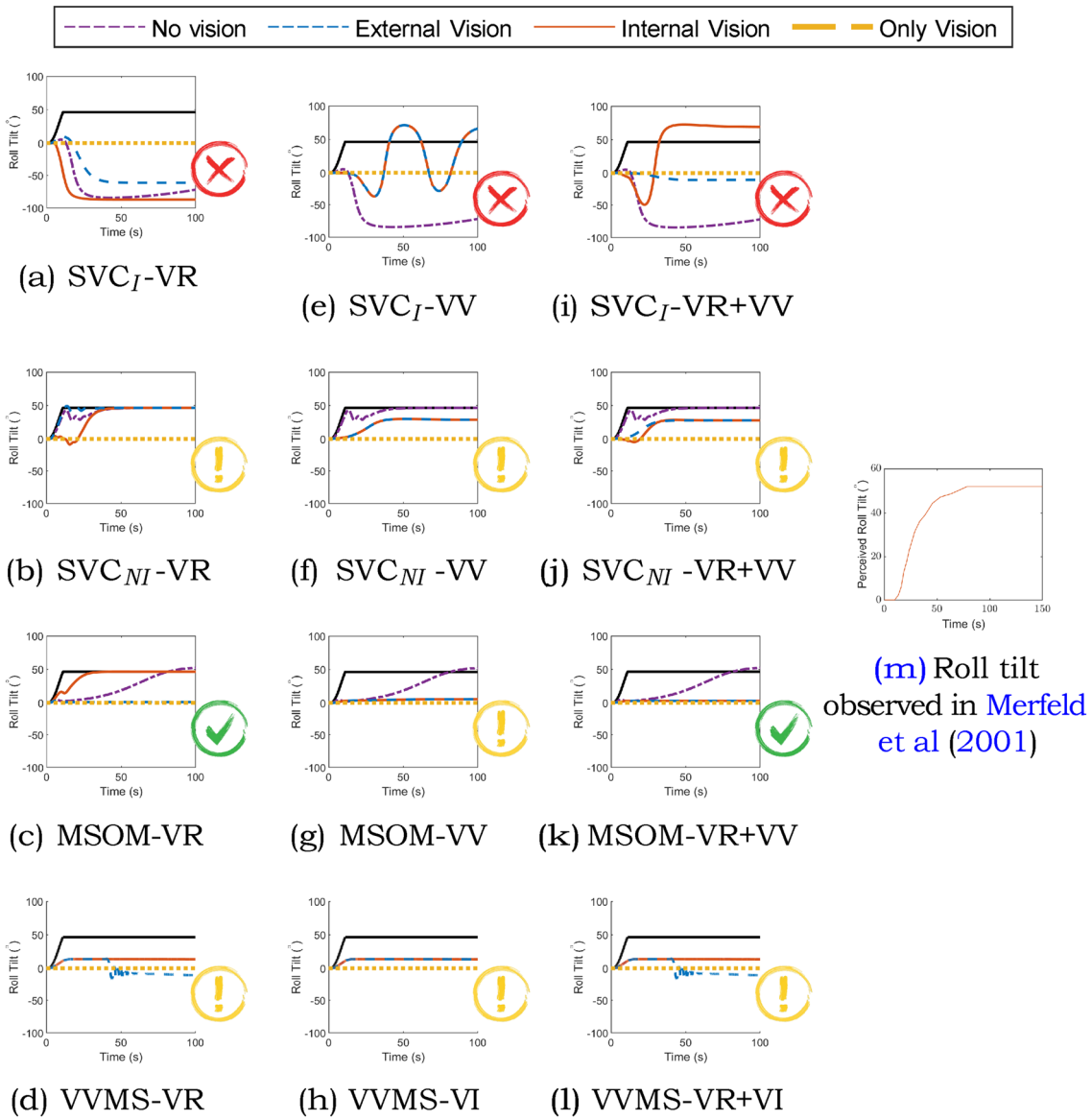

Fig. 26 Roll-tilt perception during centrifuge at 250 s^{-1}; The black lines describe the applied motion translated to an equivalent tilt angle. Red cross—result in disagreement with literature, Green Tick—result in agreement with literature, Yellow Exclamation—some of the results are in agreement with literature

vision cases. This figure is an extension of Fig. 11. Here, we present supplementary plots for the VVMS models. In the case of the VVMS model, it can be observed that the predicted conflict levels are generally lowwhen 'only' vision is considered, particularly in the VR model. Conversely, the responses for the 'external' and 'no' vision conditions are essentially identical. In contrast, the 'internal' vision condition exhibits the highest sickness levels in models with 'VI'. However, the VVMS-VR model demonstrates low conflict levels during 'internal' vision.

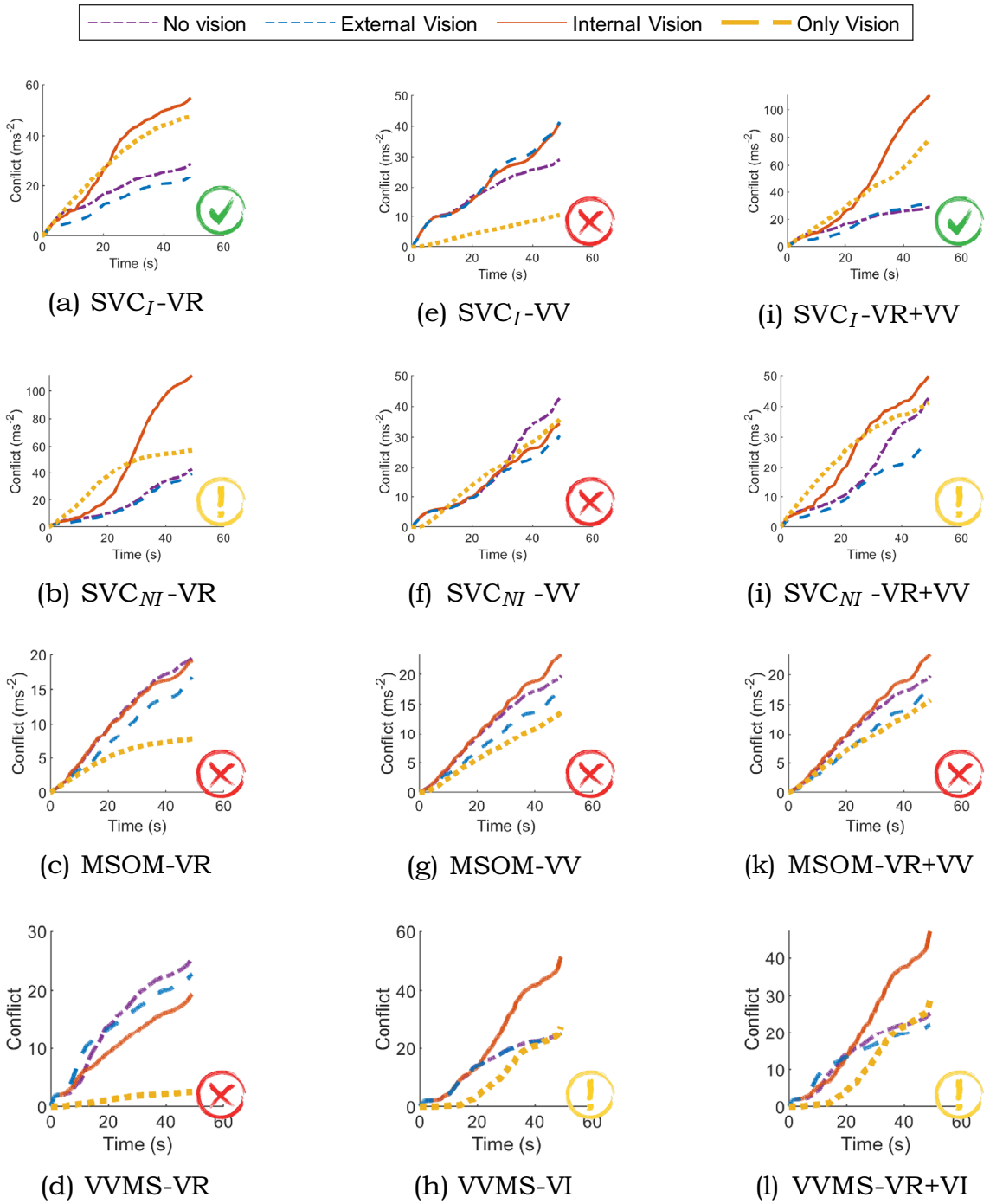

Fig. 27 Effect of vision on the accumulated conflict (ms^{-2}) for SVC$_I$, SVC$_{NI}$ and MSOM during slalom drive of 47 s for 'no', 'external', 'internal', and 'only' vision conditions; Red cross—Incorrect, Yellow Exclamation—Uncertain, Green Tick—Correct order of responses for vision conditions

Acknowledgements The contribution of Varun Kotian was financially supported by Toyota Motor Europe, and the contribution of Tugrul Irmak was supported from the European Union's Horizon 2020 research and innovation program under Grant agreement #101006664.

Data availability All data generated or analysed during this study are included in this published article (and its supplementary information files).

Declarations

Conflict of interest The authors declare that they have no conflict of interest.

Open Access This article is licensed under a Creative Commons Attribution 4.0 International License, which permits use, sharing, adaptation, distribution and reproduction in any medium or format, as long as you give appropriate credit to the original author(s) and the source, provide a link to the Creative Commons licence, and indicate if changes were made. The images or other third party material in this article are included in the article's Creative Commons licence, unless indicated otherwise in a credit line to the material. If material is not included in the article's Creative Commons licence and your intended use is not permitted by statutory regulation or exceeds the permitted use, you will need to obtain permission directly from the copyright holder. To view a copy of this licence, visit http://creativecommons.org/licenses/by/4.0/.

References

Allred AR, Clark TK (2023) A computational model of motion sickness dynamics during passive self-motion in the dark. Exp Brain Res. https://doi.org/10.1007/S00221-023-06684-9

Berger DR, Schulte-Pelkum J, Bulthoff HH (2010) Simulating believable for- ward accelerations on a stewart motion platform. ACM Trans Appl Percept (TAP). https://doi.org/10.1145/1658349.1658354

Berthoz A, Droulez J (1982) Linear self motion perception. Tutorials on motion perception. Springer, pp 157–199. https://doi.org/10.1007/978-1-4613-3569-6

Bertolini G, Straumann D (2016) Moving in a moving world: a review on vestibular motion sickness. Front Neurol. https://doi.org/10.3389/fneur.2016.00014

Bos JE, Bles W (1998) Modelling motion sickness and subjective vertical mismatch detailed for vertical motions. Brain Res Bull 47(5):537–542. https://doi.org/10.1016/s0361-9230(98)00088-4

Bos JE, Bles W, Groen EL (2008) A theory on visually induced motion sickness. Displays 29(2):47–57. https://doi.org/10.1016/j.displa.2007.09.002

Bos JE, de Vries SC, van Emmerik ML et al (2010) The effect of internal and external fields of view on visually induced motion sickness. Appl Ergon 41(4):516–521. https://doi.org/10.1016/J.APERGO.2009.11.007

Butler CA, Griffin MJ (2006) Motion sickness during fore-and-aft oscillation: effect of the visual scene. Aviat Space Environ Med 77(12):1236–1243

Cano Porras D, Zeilig G, Doniger GM et al (2020) Seeing gravity: gait adaptations to visual and physical inclines—a virtual reality study. Front Neurosci 13:1308. https://doi.org/10.3389/FNINS.2019.01308/BIBTEX

Clark TK, Newman MC, Karmali F et al (2019) Mathematical models for dynamic, multisensory spatial orientation perception. Prog Brain Res 248:65–90. https://doi.org/10.1016/BS.PBR.2019.04.014

Correia Gracio BJ, de Winkel KN, Groen EL et al (2013) The time constant of the somatogravic illusion. Exp Brain Res 224(3):313–321. https://doi.org/10.1007/s00221-012-3313-3

Dichgans J, Brandt T (2009) Optokinetic motion sickness and pseudo-coriolis effects induced by moving visual stimuli. Acta Otolaryngol 76(1–6):339–348. https://doi.org/10.3109/00016487309121519

Ehrenstein WH (2003) Basics of seeing motion. Arq Bras Oftalmol 66(5 Suppl.):44–52. https://doi.org/10.1590/S0004-27492003000600006

Golding J, Markey HM (1996) Effect of frequency of horizontal linear oscillation on motion sickness and somatogravic illusion. Aviat Space Environ Med 67(2):121–126

Golding JF, Finch MI, Stott JR (1997) Frequency effect of 0.35–1.0 Hz horizontal translational oscillation on motion sickness and the somatogravic illusion. Aviat, Space Environ Med 68(5):396–402

Golding JF, Arun S, Wortley E et al (2009) Off-vertical axis rotation of the visual field and nauseogenicity. Aviat Space Environ Med 80(6):516–521. https://doi.org/10.3357/asem.2433.2009

Griffin M, Mills K (2002a) Effect of magnitude and direction of horizontal oscillation on motion sickness. Aviat Space Environ Med 73:640–646

Griffin MJ, Mills KL (2002b) Effect of frequency and direction of horizontal oscillation on motion sickness. Aviat Space Environ Med 73(6):537–543

Griffin MJ, Newman MM (2004) Visual field effects on motion sickness in cars. Aviat Space Environ Med 75(9):739–748

Groen EL, Clark TK, Houben MMJ et al (2022) Objective evaluation of the somatogravic illusion from flight data of an airplane accident. Safety 8(4):85. https://doi.org/10.3390/SAFETY8040085

Happee R, Kotian V, de Winkel K (2023) Neck stabilization through sensory integration of vestibular and visual motion cues. Front Neurol 14(1266):345. https://doi.org/10.3389/FNEUR.2023.1266345

Howarth HVC, Griffin MJ (2003) Effect of roll oscillation frequency on motion sickness. Aviat Space Environ Med 74(4):326–331

Huppert D, Benson J, Brandt T (2017) A historical view of motion sickness—a plague at sea and on land, also with military impact. Front Neurol 8(Apr):114. https://doi.org/10.3389/FNEUR.2017.00114

Inoue S, Liu H, Wada T (2022) Revisiting motion sickness models based on SVC theory considering motion perception. SAE MobilityRxiv™ Preprint https://doi.org/10.47953/SAE-PP-00303, URL https://mobilityrxiv.sae.org/preprint/revisiting-motion-sickness-models-based-on-svc-theory-considering-motion-perception

Irmak T, Pool DM, Happee R (2020) Objective and subjective responses to motion sickness: the group and the individual. Exp Brain Res. https://doi.org/10.1007/s00221-020-05986-6

Irmak T, De Winkel KN, Pool DM et al (2021) Individual motion perception parameters and motion sickness frequency sensitivity in fore-aft motion. Exp Brain Res. https://doi.org/10.1007/s00221-021-06093-w

Irmak T, Kotian V, Happee R et al (2022) Amplitude and temporal dynamics of motion sickness. Front Syst Neurosci. https://doi.org/10.3389/FNSYS.2022.866503

Irmak T, Pool D, de Winkel K et al (2023) Validating models of sensory conflict and perception for motion sickness prediction. Biol Cybern. https://doi.org/10.1007/s00422-023-00959-8

Jalgaonkar N, Sousa Schulman D, Ojha S et al (2021) A visual-vestibular model to predict motion sickness response in passengers of autonomous vehicles. SAE Int J Adv Curr Pract Mob 3(5):2421–2432. https://doi.org/10.4271/2021-01-0104

Kamiji N, Kurata Y, Wada T et al. (2007) Modeling and validation of carsickness mechanism. In: Proceedings of the SICE Annual Conference. IEEE, pp 1138–1143, https://doi.org/10.1109/SICE.2007.4421156, http://ieeexplore.ieee.org/document/4421156/

Khalid H, Turan O, Bos JE et al (2011) Application of the subjective vertical–horizontal-conflict physiological motion sickness model to the field trials of contemporary vessels. Ocean Eng 38(1):22–33. https://doi.org/10.1016/j.oceaneng.2010.09.008

Kotian V, Pool DM, Happee R (2023) Modelling individual motion sickness accumulation in vehicles and driving simulators. In:

Proceedings of the Driving Simulation Conference, Antibes, France
Krapp HG, Hengstenberg R (1996) Estimation of self-motion by optic flow processing in single visual interneurons. Nature 384(6608):463–466. https://doi.org/10.1038/384463a0
Kufver B, Forstberg J (1999) A net dose model for development of nausea. In: (paper to) United Kingdom Group Meeting on Human Responses to Vibration, 1999, Dunton, Essex, United Kingdom, vol 330
Kuiper OX, Bos JE, Diels C (2018) Looking forward: in-vehicle auxiliary display positioning affects carsickness. Appl Ergon 68:169–175. https://doi.org/10.1016/j.apergo.2017.11.002
Liu H, Inoue S, Wada T (2022) Motion sickness modeling with visual vertical estimation and its application to autonomous personal mobility vehicles. In: 2022 IEEE Intelligent Vehicles Symposium (IV), pp 1415–1422, https://doi.org/10.1109/IV51971.2022.9827161
Mayne R (1974) A systems concept of the vestibular organs. Springer. https://doi.org/10.1007/978-3-642-65920-1
McCauley M, Royal J, Wylie C et al. (1976) Motion sickness incidence: exploratory studies of habituation, pitch and roll, and the refinement of a mathematical model. Tech. rep., Canyon Research Group Inc Goleta Ca Human Factors Research Div
Merfeld DM, Young LR, Oman CM et al (1993) A multidimensional model of the effect of gravity on the spatial orientation of the monkey. J Vestib Res 3(2):141–161. https://doi.org/10.3233/VES-1993-3204
Merfeld DM, Zupan LH, Gifford CA (2001) Neural processing of gravito-inertial cues in humans. II. Influence of the semicircular canals during eccentric rotation. J Neurophysiol 85(4):1648–1660. https://doi.org/10.1152/jn.2001.85.4.1648
Newman MC (2009) A multisensory observer model for human spatial orientation perception. PhD thesis, Massachusetts Institute of Technology, http://hdl.handle.net/1721.1/51636
O'Hanlon JF, McCauley ME (1974) Motion sickness incidence as a function of the frequency and acceleration of vertical sinusoidal motion. Aerosp Med 45(4):366–369
Oman CM (1990) Motion sickness: a synthesis and evaluation of the sensory conflict theory. Can J Physiol Pharmacol 68(2):294–303. https://doi.org/10.1139/y90-044
Reason JT (1978) Motion sickness adaptation: a neural mismatch model. J R Soc Med 71(11):819–829
Riccio GE, Stoffregen TA (2010) An ecological theory of motion sickness and postural instability. Ecol Psychol 3(3):195. https://doi.org/10.1207/s15326969eco0303_2
Salter S, Diels C, Herriotts P et al (2019) Motion sickness in automated vehicles with forward and rearward facing seating orientations. Appl Ergon 78:54–61. https://doi.org/10.1016/J.APERGO.2019.02.001
Tokumaru O, Kaida K, Ashida H et al (1998) Visual influence on the magnitude of somatogravic illusion evoked on advanced spatial disorientation demonstrator. Aviat Space Environ Med 69(2):111–116
van der Steen F (1998) Self-motion perception. PhD thesis, TU Delft, URL https://repository.tudelft.nl/islandora/object/uuid%3Adcbbad07-c8ec-437d-8b19-ff81ecfb1909
Vingerhoets RA, Medendorp WP, Van Gisbergen JA (2006) Time course and magnitude of illusory translation perception during off-vertical axis rotation. J Neurophysiol 95(3):1571–1587. https://doi.org/10.1152/JN.00613.2005
Wada T (2021) Computational model of motion sickness describing the effects of learning exogenous motion dynamics. Front Syst Neurosci 15:6. https://doi.org/10.3389/FNSYS.2021.634604/BIBTEX
Wada T, Yoshida K (2016) Effect of passengers' active head tilt and opening/closure of eyes on motion sickness in lateral acceleration environment of cars. Ergonomics 59(8):1050–1059. https://doi.org/10.1080/00140139.2015
Wada T, Kamij N, Doi S (2015) A mathematical model of motion sickness in 6DOF motion and its application to vehicle passengers. arXiv preprint http://arxiv.org/abs/1504.05261
Wada T, Kawano J, Okafuji Y et al. (2020) A computational model of motion sickness considering visual and vestibular information. In: 2020 IEEE International Conference on Systems, Man, and Cybernetics (SMC). IEEE, pp 1758–1763, https://doi.org/10.1109/SMC42975.2020.9283350
Waespe W, Henn V (1977) Neuronal activity in the vestibular nuclei of the alert monkey during vestibular and optokinetic stimulation. Exp Brain Res 27(5):523–538. https://doi.org/10.1007/BF00239041
Wood SJ (2002) Human otolith–ocular reflexes during off-vertical axis rotation: effect of frequency on tilt–translation ambiguity and motion sickness. Neurosci Lett 323(1):41–44. https://doi.org/10.1016/S0304-3940(02)00118-0
Wood SJ, Reschke MF, Sarmiento LA et al (2007) Tilt and translation motion perception during off-vertical axis rotation. Exp Brain Res 182(3):365–377. https://doi.org/10.1007/S00221-007-0994-0
Yunus I, Jerrelind J, Drugge L (2022) Evaluation of motion sickness prediction models for autonomous driving. In: Orlova A, Cole D (eds) Lecture notes in mechanical engineering. Springer International Publishing, Cham, pp 875–887. https://doi.org/10.1007/978-3-031-07305-2
Zupan LH, Merfeld DM, Darlot C (2002) Using sensory weighting to model the influence of canal, otolith and visual cues on spatial orientation and eye movements. Biol Cybern 86(3):209–230. https://doi.org/10.1007/s00422-001-0290-1

Publisher's Note Springer Nature remains neutral with regard to jurisdictional claims in published maps and institutional affiliations.